Organic Electronics 15 (2014) 3458–3464

Contents lists available at ScienceDirect

Organic Electronics

journal homepage: www.elsevier.com/locate/orgel

Bridging donor–acceptor energy offset using organic dopants as energy ladders to improve open-circuit voltages in bulk-heterojunction solar cells

Jan-Kai Chang [a], Ya-Ching Kuo [a], Yu-Jen Chen [b], An-Lun Lo [a], I-Hsiu Liu [a], Wei-Hsuan Tseng [a], Kaung-Hsiung Wu [b], Mei-Hsin Chen [c,*], Chih-I Wu [a,*]

[a] Graduate Institute of Photonics and Optoelectronics, National Taiwan University, Taipei 106, Taiwan, ROC
[b] Department of Electrophysics, National Chiao Tung University, Hsinchu 300, Taiwan, ROC
[c] Department of Opto-Electronic Engineering, National Dong Hwa University, Hualien 974, Taiwan, ROC

ARTICLE INFO

Article history:
Received 21 June 2014
Received in revised form 21 August 2014
Accepted 28 August 2014
Available online 26 September 2014

Keywords:
Organic photovoltaics
Open-circuit voltage
Ternary cascade energy alignment

ABSTRACT

A systematic way to improve the open circuit voltage of bulk-heterojunction (BHJ) organic photovoltaics is demonstrated by incorporating energy ladder material to form a ternary blend with cascade energy structures. We propose that doping organic molecules with appropriate energetic alignment to bridge the donor–acceptor energy offset can facilitate exciton dissociation and hence improve open-circuit voltage (V_{oc}) and power conversion efficiency. The cascade energy alignment structure is measured via ultraviolet photoemission spectroscopy. The V_{oc} and power conversion efficiency of devices using the proposed schemes can be enhanced by 10% and 20%, respectively. The results provide a new path toward higher power conversion efficiency in BHJ systems by engineering the energy structures of the materials in the active layers.

1. Introduction

Organic photovoltaic (OPV) devices with bulk-heterojunction (BHJ) structures are one of the promising low-cost solar cell technologies because they can be integrated into flexible substrates with minimal weight and large area [1,2]. However, the performance of OPV devices are still not as good as those of inorganic solar cells. Increasing open-circuit voltage (V_{oc}) would be one of the key steps to improve the performance of organic photovoltaic devices. Among many elements that control V_{oc}, the energy band alignments of the donor–acceptor in the BHJ devices have been reported as the major factor that limit the value of V_{oc} [3–5]. Since V_{oc} in donor–acceptor systems correlates to the energetic difference between the highest occupied molecular orbital (HOMO) of the electron donor and lowest unoccupied molecular orbital (LUMO) of the electron acceptor [6–8], one of the route toward a larger V_{oc} is to incorporate low-band gap semiconducting polymers with deeper HOMOs as donors [9,10] and electron-accepting fullerene derivatives with shallower LUMOs as acceptors [11,12]. Although many efforts have been devoted to modify the HOMO–LUMO offset of the donor–acceptor by introducing additional substituents or replacing the function group in molecules to enhance the V_{oc} of BHJ solar cells, there is normally more than 0.3 V difference between V_{oc} and the HOMO–LUMO offset. This is because a significant fraction of the photon energy (typically more than half) is given up in the rapid exciton dissociation due to the requirement of a large LUMO offset of the donor–acceptor for overcoming intramolecular Coulomb attrac-

* Corresponding authors. Tel.: +886 38634192 (M.-H. Chen), +886 233663656 (C.-I Wu).
E-mail addresses: meihsinchen@mail.ndhu.edu.tw (M.-H. Chen), chihiwu@cc.ee.ntu.edu.tw (C.-I. Wu).

http://dx.doi.org/10.1016/j.orgel.2014.08.052
1566-1199/

tion across exciton [13,14]. The current approaches for cell architecture improvement include the use of a mix solvent for interfacial morphology control, the incorporation of additives that obtain proper molecular orientation, the formation of a cascade energy structure to cover more solar spectra with ternary blend, and the addition of metal nanostructures to enhance absorption via the excited surface plasmon. These cell architecture methods have mainly been investigated for complementary absorption and better utilization of the solar radiation spectrum, particularly for improving the short-circuit current density (J_{sc}) of the BHJ solar cells [15–20]. However, the correlation between dopant and consequent V_{oc} enhancement is still ambiguous and rarely discussed. Improving power conversion efficiency (PCE) of BHJ solar cells through increasing V_{oc} values close to the theoretical maximum, the band gap of the semiconducting polymer, remains challenging.

In this paper, we demonstrate ladder-assisted BHJ solar cells with improved V_{oc} by adding the molecules with appropriate energy level alignments to bridge the energy offset between the donor and acceptor. Via *in situ* ultraviolet photoemission spectroscopy (UPS), we shows that if the HOMO level of additional hole-cascade acceptor is in-between those of donors and acceptors, the incorporation of these energy ladder materials forms a ternary cascade energy structure to bridge the energy offset of donor or acceptor, which can offer exciton dissociation paths and consequently enhances the V_{oc} of the device. The results suggest that the exciton dissociation can be assisted by traps or impurities with energetic disorder, which provides a new route toward producing a high performance BHJ solar cell through band engineering.

2. Material and methods

2.1. Material

The ITO glass purchased from Merck is 120 nm thick with a sheet resistance of approximately 25 $\Omega\,sq^{-1}$. Poly(3,4-ethylenedioxythiophene) (PEDOT) doped with poly(styrenesulfonate) (PSS) was purchased from H.C. Starck while the optically active RR-P3HT and PCBM were purchased from Rieke Metals and nano-C, respectively. The ladder materials, TCTA, is commercially available and was purchased from Sigma–Aldrich.

2.2. Methods

The solar cell structures in this study are ITO glass/PEDOT:PSS/doped P3HT:PCBM/Ca/Al. The pre-cleaned ITO substrates were first placed under UV-ozone treatment for 15 min to remove carbon and oxygen contamination absorbed during ambient transfer. Subsequently, the PEDOT:PSS (5000 rpm, ~30 nm thick) was spun-cast onto UV-ozone-treated ITO and then baked in the air at 120 °C for 15 min. The samples were then cooled to room temperature. The spin-cast P3HT:PCBM blend (25 mg:25 mg in 1 mL 1,2-dichlorobenzene) with various doping conditions (*x* mg in 1 mL 1,2-dichlorobenzene hereafter referred as *x*% dopant) was performed in a nitrogen-filled glove box and the freshly-spun active layer (600 rpm, ~230 nm thick) was allowed to dry for at least 60 min to ensure heterostructures. The samples were then annealed at 150 °C for 15 min in N_2 atmosphere before being transferred into a vacuum chamber for cathode deposition. A 20-nm calcium thin film followed by a 60-nm aluminum cathode was thermally deposited in the range of 10^{-7}–10^{-6} Torr to form 6-mm^2 doped BHJ solar cells. The doped BHJ solar cells were then characterized using a Keithley 2400 source meter under AM1.5G illumination with an irradiation intensity of 100 mW cm^{-2} in the glove box.

The EQE was performed in ambient air by QE-R-3015, Enli Technology Co., Ltd and a mono-crystalline silicon reference cell provided by Newport Corporation was used in the lamp calibration. The crystal structure of the blend films were carried out using X-ray diffraction (XRD) with a monochromatic Cu Kα radiation (λ = 1.54 Å) on a Rigaku Geigerflex diffractometer. The XRD pattern was recorded in the θ–2θ mode between 3° and 25° with a scan speed of 1° min^{-1}, operating at 40 kV and 80 mA.

The photoemission experiments were carried out in a Phi5400 system from Physical Electronics, which consists of two interconnected ultra-high vacuum chambers: one for thermal deposition and the other for spectroscopy analysis with a base pressure of 10^{-10} Torr. During the valence band ultraviolet photoemission spectra measurement with He I ($h\nu$ = 21.2 eV) as excitation sources, the samples had a bias of −5 V applied to seclude the secondary edge for the analyzer. The photoelectrons were collected using a hemispherical analyzer with an overall resolution of 0.05 eV. Doped P3HT:PCBM films for photoemission experiments were prepared under N_2 atmosphere with similar procedures for the device fabrication.

3. Results and discussion

3.1. Improved performance by incorporating energy ladder materials

In our experiments, poly (3-hexylthiophene) (P3HT) and [6,6]-phenyl-C_{61}-butyric acid methyl ester (PCBM) based BHJ solar cells are used as the baseline since they are a well-established system with efficiency of 3–4% and a stable V_{oc} of 0.6 V [21,22]. In order to bridge the energy offset of the P3HT donor and PCBM acceptor, the organic dopant should have an energy level in-between the corresponding energy band edge of the donor and acceptor to provide the cascade energy structure [23]. Fig. 1 shows the energy band alignment of P3HT and PCBM measured from UPS. To be a donor-type energy ladder, organic molecules must possess ionization energy between those of P3HT and PCBM, i.e. 4.9 and 6.1 eV, while the electron-donating ability and hole mobility must both be comparable to those of the P3HT molecules. On the other hand, we can adopt organic molecules with an electron affinity ranging from 3.0 to 3.7 eV, which are the electron affinity of P3HT and PCBM, respectively, for acceptor-type energy ladders. In addition, since imperfect phase separation generally contributes to the interfacial defect-based recombination to further limit the performance, organic dopants

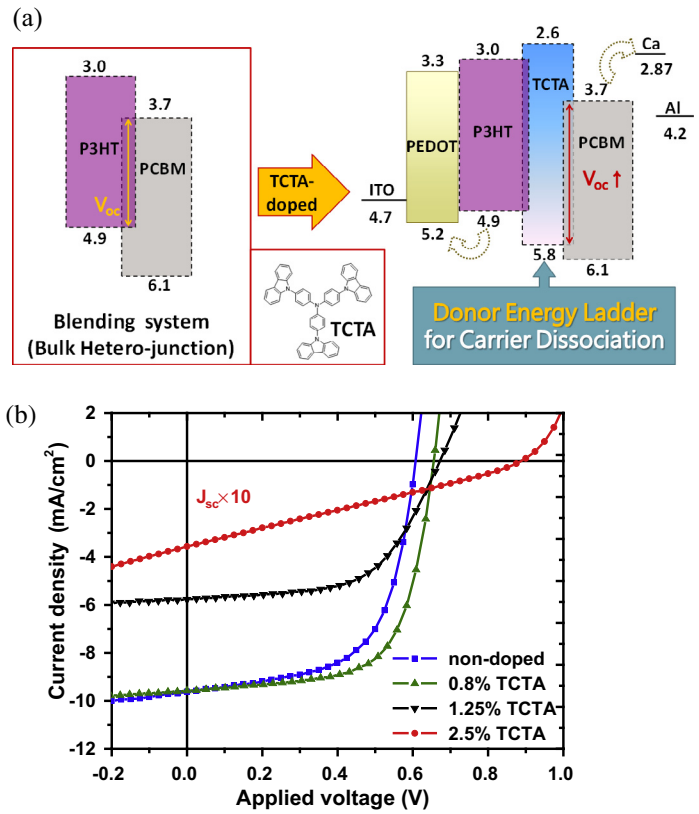

Fig. 1. Energy level diagram of the device, including ITO anode, PEDOT, photoactive P3HT:PCBM, Ca/Al cathode and dopant molecules of (a) donor-type energy ladder TCTA. (b) *J–V* characteristics corresponding to P3HT:PCBM (non-doped), P3HT:PCBM (0.8% TCTA), P3HT:PCBM (1.25% TCTA) and P3HT:PCBM (2.5% TCTA) BHJ solar cells under AM1.5G illumination with an intensity of 100 mW cm^{-2}.

possessing an excellent miscibility may be a promising candidate for the energy ladder as it will be mixed well with P3HT:PCBM and completely dissolved in 1,2-dichlorobenzene (o-DCB) to form abundant organic–organic heterojunctions with a controllable blend domain size for efficient exciton dissociation. The exciton diffusion length, which depends on the exciton mobility and exciton lifetime, is another concern when selecting proper organic dopants since the degree of exciton diffusion from the bulk domain to the donor–acceptor interface strongly affects the external quantum efficiencies (EQEs). In order to efficiently separate the photogenerated excitons into mobile electron–hole pairs, we can either introduce high-mobility organics, as has been investigated in many studies, or incorporate dopant molecules with long exciton lifetimes. The latter approach allows photogenerated excitons to reach the organic–organic heterojunction to be further dissociated.

For the aforementioned reasons, the soluble fullerene derivative, indene-C_{60} bisadduct (ICBA) has been reported as one of the best acceptor-type dopants for the energy ladder owing to its superior electron mobility and a relatively large exciton diffusion length (up to 400 Å) [24,25]. The $LUMO_{ICBA}$ is in-between $LUMO_{P3HT}$ and $LUMO_{PCBM}$, which modifies the photo-induced electron transfer and charge separation by providing an alternative path to bridge the electrons transferring from P3HT to PCBM molecules during the exciton dissociation. In this study, a hole preferential molecule, 4,4′,4″-tris-(N-carbazolyl)-triphenylamine (TCTA), is chosen as the donor-type dopant owing to the strong electron-donating ability of triphenylamine in starburst which matches that of P3HT to develop a photovoltaic effect on the heterojunctions of both P3HT:PCBM and TCTA:PCBM [26]. As illustrated in Fig. 1(a), the doped TCTA molecules with E_{HOMO} = 5.8 eV provide an intermediate energy level for exciton dissociation. The HOMO–LUMO offset is thus 2.1 eV for TCTA:PCBM heterojunctions and is larger than the original value of 1.2 eV for P3HT:PCBM heterojunctions. In addition, the promising transport ability of the hole on the TCTA molecules allows the well-separated holes moving away from the heterojunction to the bulk domain and avoids the photogenerated charges being quenched via impurity-based recombination.

To verify this idea, the P3HT:PCBM based solar cells doped with TCTA were fabricated and tested and the *J–V* characteristics are shown in Fig. 1(b). For donor energy ladder scheme, the *J–V* characteristic of TCTA doped devices based on P3HT:PCBM:TCTA = 25 mg:25 mg:8 mg in 1 mL o-DCB (hereafter referred as 0.8% TCTA) possesses a significantly improved PCE of 4.14% and a V_{oc} of 0.66 V while the V_{oc} reached 0.89 V for devices with 2.5% TCTA This result implies that the doped TCTA molecules as energy ladders

are sufficient in donating electrons to enable exciton dissociation. The relatively wide band gap of TCTA may not contribute to the absorption spectrum significantly, which is in contrast to the common ternary blend photovoltaics with an additional low band gap absorber or dye sensitization. The important parameters, such as PCE, fill factor, shunt resistance and series resistance, of these solar cells with TCTA donor ladders are summarized in Table 1.

3.2. Mechanisms of energy ladders

To further understand the mechanisms of energy ladders in BHJ solar cells, P3HT:PCBM devices doped with various TCTA concentration were studied. As shown in Fig. 2, the EQE spectra decrease upon addition of TCTA (from 8 mg to 25 mg in 1 mL o-DCB) particularly for the absorption tail and PCBM transition in the long wavelength range, indicating that the exciton dissociation at a TCTA/PCBM abundant heterojunction are not efficient. This is in addition to a lower photoelectron generated by the PCBM transition presenting a decrease at 700 nm in the EQE spectrum [27]. The result suggests that the efficiency improvement induced by the TCTA incorporation arises from energetic properties within the heterojunction, not due to the promotion in light harvesting. A proof-of-principle device with a tri-layer structure of an ultra-thin TCTA layer sandwiched between P3HT and PCBM was also created to distinguish the influence of the energy ladder since the impact of molecularly dispersed dopant molecules in BHJ devices are difficult to locate, and the *J–V* characteristic with the V_{oc} improvement (not shown here) correlates well with the observed improvement in V_{oc} in the BHJ devices containing the ladder.

A sequence of ladder-assisted P3HT:TCTA:PCBM devices with incremental composition of the donor-type energy ladder, TCTA, have also been tested to check the influence of the doping energy ladder molecules on the photovoltaic properties, and the corresponding photovoltaic parameters are summarized in Table 1. The detailed dependence of photovoltaic parameters on doping ratio for ladder-assisted P3HT:TCTA:PCBM devices is shown in Fig. 3. Note that the indication of *x* in TCTA ratio herein represents a BHJ solar cell structure of ITO glass/PEDOT:PSS/doped P3HT:PCBM/Ca/Al, where the doped P3HT:PCBM is formed by an o-DCB solvent composed of P3HT:PCBM:TCTA blend in 1:1:*x* ratio. As can be seen in Fig. 3(a), it is apparent that the V_{oc} of the ladder-assisted P3HT:TCTA:PCBM device increased with TCTA doping ratio, leading to a maximum value of 0.89 V for the TCTA-doped device rather than the pristine value of 0.6 V for the P3HT:PCBM blend. This result shows that the exciton dissociation process evolves into ladder-assisted dissociation by expanding the HOMO–LUMO offset with abundant TCTA:PCBM heterojunctions, additionally contributing to the energy-gradient-driven intermolecular hopping to lessen the energy loss during ultrafast quasi-adiabatic charge transfer at the donor–acceptor interface. Thus, the V_{oc} of the ladder-assisted P3HT:TCTA:PCBM device is improved. However, the introduction of TCTA energy ladders into the active blend also modifies the J_{sc}. Its dependence on the doping ratio shows a reverse dependency as compared to V_{oc}. In small fractions of TCTA the reduction in J_{sc} is only of 5%, while incorporating a large amount of TCTA (herein referred to as a TCTA ratio >0.5) significantly reduces J_{sc} with an over 10-fold photocurrent loss. This large reduction in J_{sc} might either relate to the reduction in photo-induced exciton when the wide-band-gap TCTA energy ladders are substituted for the photoactive P3HT or be due to the low absorption coefficient of PCBM to form the inefficient charge transfer in the heterojunction system. In addition, if the doping of the TCTA energy ladders is too heavy to diminish the impurity-based recombination, the difference of three orders of magnitude in hole mobility between TCTA and P3HT can deliver mobility disorder to greatly quench the free charge carriers. In this way, the lack of percolation channels for charge transport and separation resulting from the lower degree of active matrix induced by excess TCTA molecules may drastically decrease the photocurrent, which is correlated well with the EQE spectra in Fig. 2.

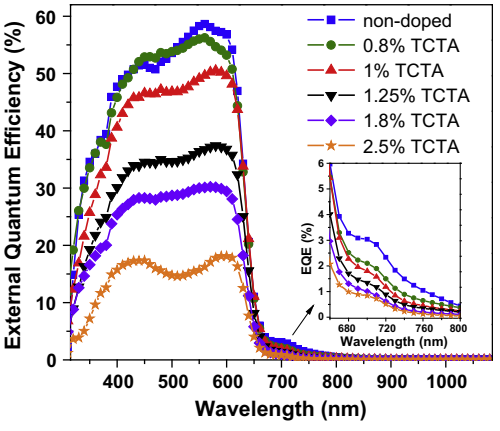

Fig. 2. EQE spectra of the ladder-assisted BHJ solar cell including 0% (■), 0.8% (●), 1% (▲), 1.25% (▼), 1.8% (♦), 2.5% (★) TCTA. The EQE spectra between 660 and 800 are enlarged as inset.

In Fig. 3(b) the non-linearity correlation between either the PCE or *FF* and the doping ratio of TCTA in the ladder-assisted P3HT:TCTA:PCBM devices is shown. The doping-related *FF* and PCE values passed through a typical maximum around a doping ratio of 0.3 and then abruptly dropped as the TCTA dominates the P3HT in the BHJ system. This is not only caused by the interplay between V_{oc} and J_{sc}, but also due to inefficient photo-induced electron transfer from P3HT to PCBM which is attributed to the smaller electron affinity of TCTA than that of P3HT and PCBM. Hence for heavy doped devices, it is reasonable to assume that the abundance of TCTA molecules within the phase-separated networks of P3HT:PCBM act as an intermediate energy barrier to mobile electrons, or, in another words, the P3HT molecules surrounded by TCTA serve as trap sites. The hindering of photo-induced electron transfer from P3HT to PCBM through photo-induced hole transfer from PCBM to TCTA is to be expected. In general, we observe a reduction of the *FF* and photocurrent in heavy-doped devices, which indicates a reduced level of absorption and exciton dissociation in dopant molecules with

Table 1
Operating parameters of OPV devices incorporating TCTA donor energy ladder.

Device	PCE (%)	V_{oc} (V)	J_{sc} (mA cm^{-2})	*FF* (%)	R_s (Ω cm^2)	R_{sh} (Ω cm^2)
P3HT:PCBM	3.54	0.60	9.74	60.2	8.33	564.8
0.8% TCTA doped	4.14	0.66	9.48	66.7	9.78	960.4
1.25% TCTA doped	2.25	0.68	5.77	57.6	28.07	1176.2
2.5% TCTA doped	0.10	0.89	0.36	31.2	985.71	2467.4

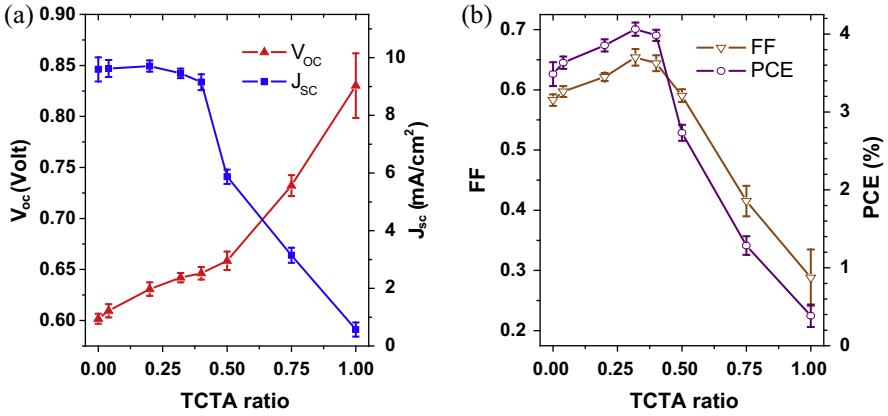

Fig. 3. Evolution of photovoltaic parameters, (a) V_{oc}, J_{sc} and (b) *FF*, PCE, for doped P3HT:PCBM BHJ solar cell incorporating different content of TCTA as donor-type energy ladder.

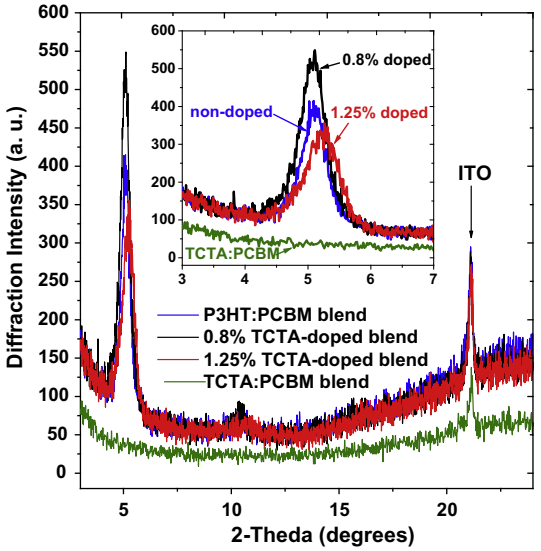

Fig. 4. XRD spectra of pristine P3HT:PCBM, P3HT:PCBM (0.8% TCTA-doped), P3HT:PCBM (1.25% TCTA-doped) and TCTA:PCBM blend, where the peak at $2\theta = 5°$ is corresponding to the interchain spacing in P3HT associated with the interdigitated alkyl chains and the peak at $2\theta = 22°$ is due to diffractions from ITO (211). The inset shows the region around $2\theta = 5°$ in greater detail.

additional loss of free charge carriers due to the trapping effects via P3HT.

X-ray diffraction (XRD) was performed in order to check the phase-separated networks in the doped active blend. The XRD results are shown in Fig. 4 and indicate a variety in the crystallinity of the active layer while the signal corresponding to ITO (211) remains constant for BHJ solar cells incorporating different amounts of the TCTA energy ladder, suggesting that the TCTA molecules penetrated the space between the polymer side chains to modify the P3HT domain size. Increased intensity of the peak at $2\theta = 5°$ with moderate doping infers that the presence of the TCTA energy ladder improves the crystallinity within the phase-separated networks and thereby facilitates exciton dissociation [28]. This in turn leads to a more periodic and self-organized crystalline structure for P3HT:TCTA:PCBM film, facilitating the intrinsic π–π stacking and charge transfer to improve the device performance. On the other hand, since considerable TCTA molecules intrude into the interchain spacing in the P3HT to deteriorate the crystallinity, the decreased intensity caused by incomplete phase separation is observed in the XRD spectrum of the over-doped active blend, resulting in rising series resistance, R_s, which greatly limits the photocurrent as indicated in Table 1. Furthermore, the improvement of shunt resistance, R_{sh}, accompanying the doping energy ladder is consistent with a greater selectivity in harvesting well-separated charge carriers and the improved V_{oc} of the ladder-assisted P3HT:TCTA:PCBM devices. This is a further evidence to conclude that the exciton-dissociated hole transport to P3HT is improved by utilizing TCTA as an energy ladder, whereas the undesirable reverse transfer of electrons is blocked by the low LUMO energy of TCTA to diminish the shunt path.

We have shown that the improved crystallinity by incorporating TCTA, which should promote a reduction in shunt loss and efficient charge generation, is commensurate with

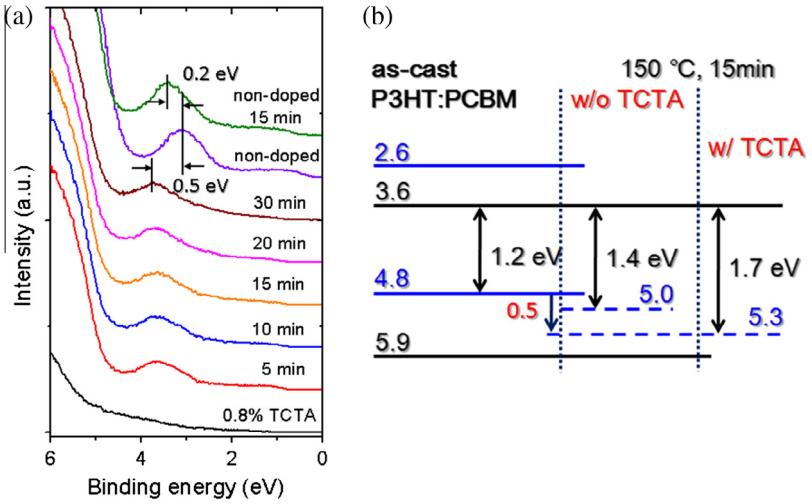

Fig. 5. (a) UPS spectra for pristine and 0.8% TCTA doped P3HT:PCBM blend with different annealing duration at 150 °C. (b) Energy band diagram deduced from the UPS spectra. The units are in eV and are w.r.t vacuum level. The blue lines indicate the LUMO and HOMO of P3HT while the black lines represent the energy levels of PCBM. (For interpretation of the references to color in this figure legend, the reader is referred to the web version of this article.)

the observed improvement in *FF* for the ladder-containing devices. To verify the observed enhancement of V_{oc} is associated to the energy level alignments, the energetic attributes of the energy ladder are further investigated via UPS. Comparison of the results via the UPS spectra of the doped blend (as indicated in the bottom of Fig. 5(a)) with corresponding data from the pristine blend, which are naturally sensitive to the composed heterojunction within the top 20-Å surface, provides direct evidence of the top TCTA-rich surface for the doped blend instead of the top P3HT-rich surface addressed in previous work [4]. As established in the earlier study, thermally induced out-diffusion of PCBM molecules to the top surface improves the transport across the heterojunction and shows a HOMO shift of 0.2 eV in the UPS spectrum under thermal annealing [29]. We note that the UPS spectra shown here present an apparent variation in the HOMO structure with an additional peak occurring at 3.7 eV after *in situ* heating of the doped blend to 150 °C, which suggests that the out-diffusion of the PCBM molecules takes place for the doped blend as well. This leaves the TCTA energy ladder sandwiched between the P3HT:PCBM as the likely candidate to bridge the donor–acceptor HOMO offset to develop an energetic favorable alignment. The thermally induced peak shift for the ladder-assisted blend exhibits a 0.5 eV shift toward a higher binding energy, larger than that of the pristine P3HT:PCBM blend. Accordingly, the evolution of energy alignment deduced from the UPS data as shown in Fig. 5(b) indicates that incorporation of the TCTA energy ladder extends the HOMO–LUMO offset between the donor and acceptor, leading to an increase in V_{oc} for the ladder-assisted P3HT:TCTA:PCBM devices.

4. Conclusion

In conclusion, unlike the conventional aim of ternary incorporation to generate complementary absorption of the solar radiation spectrum, we have proposed that the V_{oc} of a BHJ solar cell can be improved through bridging of the donor–acceptor energy offset by doping organic molecules with appropriate energetic alignment even though the dopant molecules would not help in light absorption. The energetic role of the energy ladder and the bridging mechanism within the BHJ device has been investigated in detail. It was suggested that exciton dissociation can be trap or impurity assisted with energetic disorder. From the XRD results, incorporation of the TCTA energy ladder increased the crystallinity within the phase-separated networks diminishing the shunt loss to facilitate ladder-assisted dissociation. According to the UPS results, the origin of the V_{oc} improvement in the doped device has been attributed to a rather energetic favorable dissociation, which altered the dissociation properties of the photogenerated exciton by doping the energy ladder and lessened the energy loss during ultrafast quasi-adiabatic charge transfer at the donor–acceptor interface to yield the mobile hole on the donor and electron on the acceptor. The overall impact of the bridging mechanism introduced by the TCTA energy ladder was optimized, which allows over 10% improvement in the PCE and V_{oc} for the ladder-assisted P3HT:TCTA:PCBM devices (4.14% of PCE and 0.66 V of V_{oc}) in comparison to the pristine device (3.54% of PCE and 0.60 V of V_{oc}). This 17% net increase in PCE coupled to energetic favorable alignment from the incorporation of the energy ladder with specific properties demonstrates the crucial role of interface modification in the BHJ devices.

Acknowledgements

The authors thank Yun-Hua Hong for informative discussions. This research was financially supported by the National Science Council of the Republic of China (Contract Nos. NSC 100-3113-E-002-012 and NSC 101-3113-E-002-010) and the Center for Emerging Materials and Advanced Devices, National Taiwan University.

References

[1] G. Dennler, M.C. Scharber, C.J. Brabec, Adv. Mater. 21 (2009) 1323.
[2] C.J. Brabec, S. Gowrisanker, J.J.M. Halls, D. Laird, S. Jia, S.P. Williams, Adv. Mater. 22 (2010) 3839.
[3] W.L. Leong, S.R. Cowan, A.J. Heeger, Adv. Energy Mater. 1 (2011) 517.
[4] W.H. Tseng, M.H. Chen, J.Y. Wang, C.T. Tseng, H. Lo, P.S. Wang, C.I. Wu, Sol. Energy Mater. Sol. Cells 95 (2011) 3424.
[5] P. Schlinsky, C. Waldauf, C.J. Brabec, Appl. Phys. Lett. 81 (2002) 3885.
[6] M.C. Scharber, D. Wuhlbacher, M. Koppe, P. Denk, C. Waldauf, A.J. Heeger, C.J. Brabec, Adv. Mater. 18 (2006) 789.
[7] C.J. Brabec, A. Cravino, D. Meissner, N.S. Sariciftci, T. Fromherz, M.T. Rispens, L. Sanchez, J.C. Hummelen, Adv. Funct. Mater. 11 (2011) 374.
[8] B.P. Rand, D.P. Burk, S.R. Forrest, Phys. Rev. B 75 (2007) 115327.
[9] S.H. Park, A. Roy, S. Beaupré, S. Cho, N. Coates, J.S. Moon, D. Moses, M. Leclerc, K. Lee, A.J. Heeger, Nat. Photonics 3 (2009) 297.
[10] H. Chen, J. Hou, S. Zhang, Y. Liang, G. Yang, Y. Yang, L. Yu, Y. Wu, G. Li, Nat. Photonics 3 (2009) 649.
[11] G. Zhao, Y. He, Y. Li, Adv. Mater. 22 (2010) 4355.
[12] H.C. Hesse, J. Weickert, C. Hundschell, X. Feng, K. Müllen, B. Nickel, A.J. Mozer, L. Schmidt-Mende, Adv. Energy Mater. 1 (2011) 861.
[13] M.C. Scharber, D. Mühlbacher, M. Koppe, P. Denk, C. Waldauf, A.J. Heeger, C.J. Brabec, Adv. Mater. 18 (2006) 789.
[14] A.A. Bakulin, A. Rao, V.G. Pavelyev, P.H.M. van Loosdrecht, M.S. Pshenichnikov, D. Niedzialek, J. Cornil, D. Beljonne, R.H. Friend, Science 335 (2012) 1340.
[15] S. Alem, T.Y. Chu, S.C. Tse, S. Wakim, J. Lu, R. Movileanu, Y. Tao, F. Bélanger, D. Désilets, S. Beaupré, M. Leclerc, S. Rodman, D. Waller, R. Gaudiana, Org. Electron. 12 (2011) 1788.
[16] J. Peet, J.Y. Kim, N.E. Coates, W.L. Ma, D. Moses, A.J. Heeger, G.C. Bazan, Nat. Mater. 6 (2007) 497.
[17] H.A. Atwater, A. Polman, Nat. Mater. 9 (2010) 205.
[18] H.J. Cha, D.S. Chung, S.Y. Bae, M.J. Lee, T.K. An, J.H. Hwang, K.H. Kim, Y.H. Kim, D.H. Choi, C.E. Park, Adv. Funct. Mater. 23 (2013) 1556.
[19] J.S. Huang, T. Goh, X. Li, M.Y. Sfeir, E.A. Bielinski, S. Tomasulo, M.L. Lee, N. Hazari, A.D. Taylor, Nat. Photonics 7 (2013) 479.
[20] H. Xu, T. Wada, H. Ohkita, H. Benten, S. Ito, Electrochim. Acta 100 (2013) 214.
[21] W.H. Tseng, M.H. Chen, C.C. Chang, W.H. Lin, L.C. Chen, K.H. Chen, C.I. Wu, Thin Solid Films 520 (2012) 5413.
[22] F. Padinger, R.S. Rittbegber, N.S. Sariciftci, Adv. Funct. Mater. 13 (2013) 85.
[23] T. Ameri, P. Khoram, J. Min, C.J. Brabec, Adv. Mater. 25 (2013) 4245.
[24] P. Cheng, Y. Li, X. Zhan, Energy Environ. Sci. 7 (2014) 2005.
[25] Q. An, F. Zhang, L. Li, Z. Zhou, J. Zhang, W. Tang, F. Teng, Phys. Chem. Chem. Phys. 16 (2014) 16103.
[26] B.P. Rand, D.P. Burk, S.R. Forrest, Adv. Mater. 6 (1994) 677.
[27] M. Presselt, F. Herrmann, S. Shokhovets, H. Hoppe, E. Runge, G. Gobsch, Chem. Phys. Lett. 542 (2012) 70.
[28] W. Ma, C. Yang, X. Gong, K. Lee, A.J. Heeger, Adv. Funct. Mater. 15 (2005) 1617.
[29] W.H. Tseng, H. Lo, J.K. Chang, I.H. Liu, M.H. Chen, C.I. Wu, Appl. Phys. Lett. 103 (2013) 183506.